Metastable dodecagonal-atomic-column state related to the formation of the σ structure in the Cr-Co alloy system

Toshihiro Doi,[1] Makoto Tanimura,[2] and Yasumasa Koyama[1]
[1]*Department of Electronic and Photonic Systems and Kagami Memorial Laboratory for Materials Science and Technology, Waseda University, Shinjuku, Tokyo 169-8555, Japan*
[2]*Research Department, NISSAN ARC, Limited, Yokosuka, Kanagawa 237-0061, Japan*
(Received 2 December 2008; published 22 April 2009)

The σ phase in transition-metal alloy systems such as the Fe-Cr and Cr-Co systems has a very complicated crystal structure consisting of complex coordination polyhedra including polyhedra with coordination number 14. To understand the structural unit of the σ structure, we have examined the crystallographic features of the (bcc$\rightarrow$bcc+σ) reaction in the Cr-Co alloy system by transmission electron microscopy. It was, as a result, found that there existed a metastable state consisting of dodecagonal atomic columns, which are entirely different from atomic columns produced by a one-dimensional connection of polyhedra with coordination number 14. The (bcc$\rightarrow\sigma$) structural change, in fact, occurred via the metastable dodecagonal-atomic-column lattice (DACL) state. In an ideal case, the DACL state is characterized by a periodic array of dodecagonal atomic columns. The interesting features of the structural change are that dodecagonal atomic columns are already present in the bcc matrix, and that the change from the DACL state to the σ structure is associated with the formation of polyhedra with coordination number 12 in a metastable precipitate, which are also involved in the σ structure. A polyhedron with coordination number 12 is obviously an icosahedral atomic cluster. It is thus understood that an icosahedral atomic cluster is identified as a structural unit of the σ structure.

DOI: 10.1103/PhysRevB.79.134204 PACS number(s): 71.20.Lp, 68.37.Lp, 71.20.Be

I. INTRODUCTION

In industrial applications, the σ phase in transition-metal alloys such as Fe-Cr and Cr-Co alloys is known to be an unfavorable intermetallic-compound phase because of its brittleness.[1–5] The σ phase has a complicated crystal structure involving complex coordination polyhedra like the Laves, μ, and R phases.[6–11] Figure 1 shows a schematic diagram of the $[001]_\sigma$ projection for the crystal structure of the σ phase in the Cr-Co alloy system as reported by Dinkins and co-workers.[12] As shown in the projection, the interesting feature of the σ structure is that, in addition to the presence of the α- and β-type polyhedra with coordination number (CN) 12, that is, icosahedral atomic clusters, a one-dimensional connection of polyhedra with CN 14 along the $[001]_\sigma$ direction produces an atomic column with the column axis parallel to a mixed-site chain. This tells us that the σ structure is characterized by a periodic array of this kind of atomic columns. Although a CN14 column may be identified as a structural unit of the σ structure, this suggestion has not been confirmed yet. Note that the α-type CN12 polyhedron is just rotated by 90 degrees about the $[001]_\sigma$ direction from the β-type one.

Prior to the study of the σ structure, our interest was focused on the formation of both the $MgZn_2$-type (C14) and $MgCu_2$-type (C15) Laves structures from the bcc structure. It is known that the Laves phases have crystal structures consisting mainly of icosahedral atomic clusters (CN12 polyhedra).[4,5] We had examined the crystallographic features of metastable states appearing during the formation of these two structures in Ti-Cr and Fe-Mo alloy systems by transmission electron microscopy.[13,14] As a result, it was found that the C15 structure in the former Ti-Cr alloy system consisted of decagonal atomic columns constructed by connecting icosahedral atomic clusters along the $[110]_{C15}$ direction, and that the disordered decagonal-atomic-column state appeared as a metastable state related to the formation of the C14 structure in the latter system. We also suggested that Cr-Cr and Fe-Fe atomic bonds with covalent character were, respectively, formed along column axes of decagonal atomic columns in the Ti-Cr and Fe-Mo alloys. Based on these findings, it is likely that the formation of complex CN-polyhedra structures is directly associated with the development of a three-dimensional covalent network in transition-metal alloys.

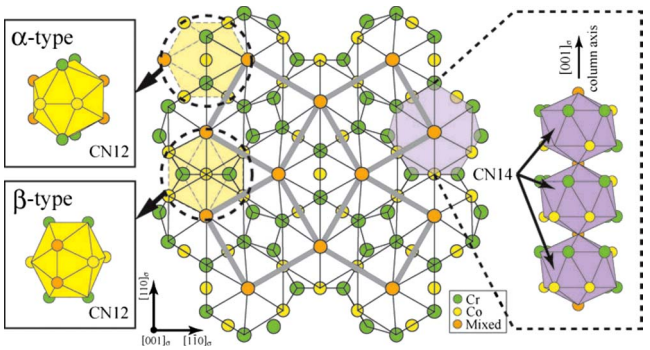

FIG. 1. (Color online) $[001]_\sigma$ projection of the reported crystal structure of the σ phase in the Cr-Co alloy system. The three-dimensional schematic diagram for both an atomic column consisting of CN14 polyhedra (purple color) and two types of CN12 polyhedra (yellow color) involved in the structure are also depicted on the right and left sides, respectively. The column axis of a CN14 column is parallel to the $[001]_\sigma$ direction, and the α- and β-type CN12 polyhedra are present in the σ structure. The difference between these two CN12 polyhedra is just a crystallographic orientation about the $[001]_\sigma$ direction.

As was mentioned above, decagonal atomic columns appeared as a metastable state in the formation process of the Laves structures. This may be indicative of the fact that the σ structure is also one of the atomic-column structures in transition-metal alloys, and that its column consists of CN14 polyhedra. Atomic bonding with covalent character is likely to form along a column axis in the atomic column. With this motivation, we have examined the crystallographic features of metastable states appearing in the formation process of the σ structure from the bcc structure, using a metastable-bcc Cr-24 at. % Co alloy. Note that according to the reported phase diagram,[15,16] the stable σ phase is present at around 40 at. % Co, with a relatively large Co-composition range. To thoroughly examine the crystallographic features of the formation of the σ structure, metastable-bcc Cr-24 at. % Co alloy samples were kept at two temperatures, 1073 and 1173 K for the (bcc $\rightarrow$ bcc+σ) reaction. In this study, the experimental data have been collected mainly from alloy samples annealed at 1173 K, while the data from samples annealed at 1073 K were used to confirm the data from the 1173 K annealed samples. Surprisingly, a careful analysis of experimental data obtained in this study clearly indicates that dodecagonal atomic columns having two shells, which are distinct from CN14 columns, appeared as a metastable state. The detailed features of experimental data including the dodecagonal atomic column found in this study will be described below.

II. EXPERIMENTAL PROCEDURE

Ingots of Cr-24 at. % Co alloy were prepared from Cr and Co of 99.9% purity by an Ar arc melting technique. The ingots were kept at 1673 K in the bcc region for 24 h, followed by quenching in ice water. To induce the (bcc $\rightarrow$ bcc +σ) reaction, metastable-bcc alloy samples cut from the ingots were annealed at 1073 and 1173 K in vacuum for various annealing times, and then quenched in ice water. The crystallographic features of each annealed sample were examined at room temperature, using JEM-3010 and 1010-type transmission electron microscopes with accelerating voltages of 300 and 100 kV, respectively. Specimens for our observation were prepared by an Ar-ion thinning technique.

III. EXPERIMENTAL RESULTS

Before describing the crystallographic features in the formation process of the σ structure from the bcc structure, including the appearance of a dodecagonal atomic column found in this study, we first report the experimental results on the orientation relationship between the bcc and σ structures. The relationship was actually determined by using equilibrium samples annealed for more than 24 h. Figure 2 shows, as an example, a bright-field image and three corresponding electron-diffraction patterns of an equilibrium Cr-24 at. % Co alloy sample annealed at 1173 K for 24 h. The electron incidences of the patterns in (b), (c), and (d) are, respectively, parallel to $[113]_{bcc}$, $[33\bar{2}]_{bcc}$, and $[1\bar{1}0]_{bcc}$ directions, while the image in (a) was taken at the $[113]_{bcc}$ incidence. A σ precipitate observed as a faint dark contrast is

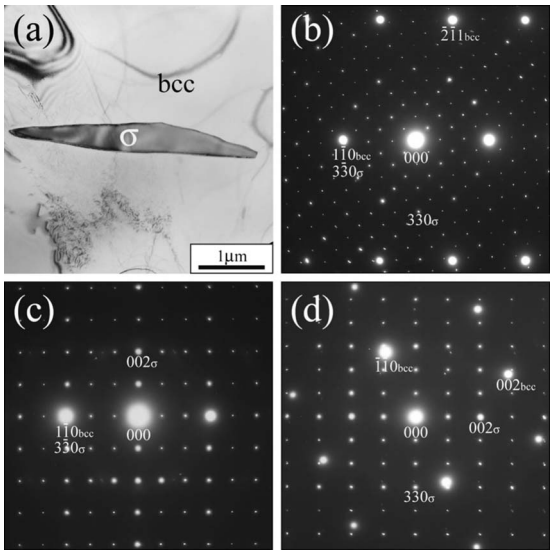

FIG. 2. Bright-field image and three electron-diffraction patterns taken from an equilibrium Cr 24 at.% Co alloy sample annealed at 1173 K for 24 h. A large σ precipitate at the center of the image is present in a bcc matrix. The patterns with the (a) $[113]_{bcc}$, (b) $[33\bar{2}]_{bcc}$, and (c) $[1\bar{1}0]_{bcc}$ electron incidences indicate that there is the orientation relation of $[113]_{bcc}\|[001]_{\sigma}$ and $(1\bar{1}0)_{bcc}\|(3\bar{3}0)_{\sigma}$ between the bcc and σ structures. This relation is referred to as the (IA) relation in this study.

present in a surrounding bcc matrix, and its size is estimated to be about 0.5 and 4.0 nm, respectively, in the vertical and horizontal directions of the image. In the diffraction patterns, on the other hand, there are strong reflections due to the bcc matrix, while the σ precipitate gives rise to weak reflections. The points to note here are that locations of weak σ reflections in (b), (c), and (d) correspond to those in the $[001]_{\sigma}$, $[110]_{\sigma}$, and $[1\bar{1}0]_{\sigma}$ patterns of the σ structure, respectively, and that the location of the $1\bar{1}0_{bcc}$ reflection is identical to that of the $3\bar{3}0_{\sigma}$ reflection in (b) and (c). This clearly indicates the existence of the orientation relation of $[113]_{bcc}\|[001]_{\sigma}$ and $(1\bar{1}0)_{bcc}\|(3\bar{3}0)_{\sigma}$.

Our experimental data obtained in this study were found to establish the presence of five orientation relations between the bcc and σ structures, including the above-mentioned relation. The notable feature of these relations is that they are classified into three groups with respect to the $[001]_{\sigma}$ direction of the σ structure; that is, (I) $[113]_{bcc}\|[001]_{\sigma}$, (II) $[111]_{bcc}\|[001]_{\sigma}$, and (III) $[110]_{bcc}\|[001]_{\sigma}$. Five electron-diffraction patterns indicating these relations are shown in Fig. 3. The patterns in (a) and (a′), (b), and (c) and (c′), respectively, have the $[113]_{bcc}$, $[111]_{bcc}$, and $[110]_{bcc}$ electron incidences, which are parallel to the $[001]_{\sigma}$ direction in each group. Among these patterns, we look first at the patterns with the $[113]_{bcc}$ incidence in (a) and (a′) for the (I) group. Note that the pattern in (a) is the same as that in Fig. 2(b). The features of the patterns are that, as mentioned above, the location of the $1\bar{1}0_{bcc}$ reflection is identical to that of the $3\bar{3}0_{\sigma}$ reflection in (a), while the locations of the $1\bar{1}0_{bcc}$ and $4\bar{1}0_{\sigma}$ reflections are almost the same as in (a′). This give us

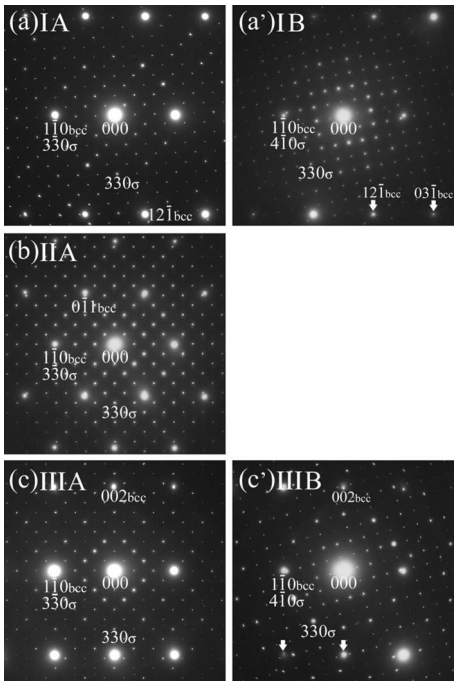

FIG. 3. Electron-diffraction patterns indicating five orientation relations between the bcc and σ structures. The five relations are classified into three groups. There are the (IA) and (IB) relations in the (I) group, (a) and (a′), the (IIA) relation in the (II) group, (b), and the (IIIA) and (IIIB) relations in the (III) group, (c) and (c′). The notable feature of the relations is that Bragg conditions of some reflections are not fully satisfied, in particular, as indicated by the arrows in (a′) and (c′). Based on this, we know that there is some deviation of the orientation relation in each case.

two relations for (IA) $[113]_{bcc}\|[001]_{\sigma}$, $(1\bar{1}0)_{bcc}\|(3\bar{3}0)_{\sigma}$ and for (IB) $[113]_{bcc}\|[001]_{\sigma}$, $(1\bar{1}0)_{bcc}\|(4\bar{1}0)_{\sigma}$. In the (II) group, there exists the relation of (IIA) $[111]_{bcc}\|[001]_{\sigma}$, $(1\bar{1}0)_{bcc}\|(3\bar{3}0)_{\sigma}$ because of the same locations of the $1\bar{1}0_{bcc}$ and $3\bar{3}0_{\sigma}$ reflections in (b). As for the (III) group, moreover, the patterns in (c) and (c′) lead to two more relations for (IIIA) $[110]_{bcc}\|[001]_{\sigma}$, $(1\bar{1}0)_{bcc}\|(3\bar{3}0)_{\sigma}$ and for (IIIB) $[110]_{bcc}\|[001]_{\sigma}$, $(1\bar{1}0)_{bcc}\|(4\bar{1}0)_{\sigma}$. Note that the above-determined relations are rather approximate, and that some slight deviation from the relation in each case is also detected, particularly in (a′) and (c′). In (a′), for instance, the Bragg conditions of the $12\bar{1}_{bcc}$ and $03\bar{1}_{bcc}$ reflections are not fully satisfied, as indicated by the arrows. The presence of the five orientation relations is very surprising to us. We thus speculate that both the five relations and some slight deviation in each case are indicative that a hidden state should be present as a metastable state. To find such a state, we examined the detailed features of the formation process of the σ structure from the bcc structure.

In this study, the crystallographic features of the formation of the σ structure were examined by taking high-resolution electron micrographs of annealed samples. The notable feature of our analysis is that we did not get the structural information directly from micrographs obtained experimentally, but from calculated micrographs reproduced

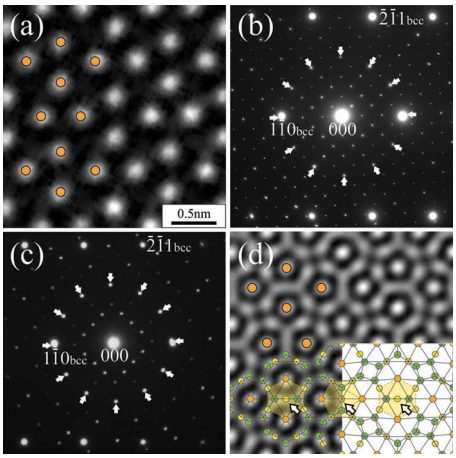

FIG. 4. (Color online) High-resolution electron micrograph, two $[001]_{\sigma}$ electron-diffraction patterns, and a calculated micrograph to explain the method of our analysis for high-resolution electron micrographs obtained from annealed samples. Both the micrograph in (a) and the corresponding pattern in (b) were taken from an equilibrium Cr-24 at. % Co alloy sample annealed at 1173 K for 24 h. The defocus value and the sample thickness for the experimental micrograph in (a) are, respectively, estimated to be about −60 nm and about 25 nm. Note that the same experimental condition was basically used for the other micrographs shown in this paper. Although the pattern in (b) exhibits 12 reflections with a pseudo-12-fold symmetry around the origin 000, as indicated by the solid arrows, only a regular array of bright dots corresponding to center positions (orange color) of CN14 columns are seen in the experimental micrograph. As the 12 reflections are also observed in the pattern (c) of a metastable sample annealed at 1173 K for 10 min, we produced the calculated micrograph in (d) by using only these 12 reflections. In spite of the involvement of only the 12 reflections, surprisingly, the calculated micrograph can reproduce the essential features of the σ structure.

by using some reflections in diffraction patterns. To obtain the crystallographic features in the $[001]_{\sigma}$ projection, in particular, we used calculated micrographs reproduced by 12 reflections in the $[001]_{\sigma}$ diffraction pattern, which were arranged with a pseudo-12-fold symmetry around the origin 000. In Fig. 4, for example, a high-resolution electron micrograph, two diffraction patterns, and a calculated micrograph are shown to explain the background of this approach. Figures 4(a) and 4(b) are, respectively, a high-resolution electron micrograph and a corresponding $[001]_{\sigma}$ electron-diffraction pattern of an equilibrium sample annealed at 1173 K for 24 h, while the pattern in (c) is from a sample annealed at 1173 K for 10 min. Note that the pattern of the latter sample with the short annealing time should reflect the crystallographic features of a metastable state in an early stage of the (bcc $\rightarrow \sigma$) structural change. In the micrograph (a) of the equilibrium state, first, a regular array of bright dots is clearly seen, as marked by the orange-color dots. The image simulation based on the σ structure in Fig. 1 indicated that each bright dot corresponded to a center position of a CN14 atomic column. In other words, the experimental micrograph in (a) emphasizes mainly an array of CN14 columns, but it is hard to understand the detailed features of the σ structure in the $[001]_{\sigma}$ projection. We then look for a change in electron-

diffraction patterns during the structural change. From the comparison between the diffraction patterns in (b) and (c), we see that 12 reflections indicated by the solid arrows are already present in the early stage. This may imply that a certain structural unit giving rise to 12 reflections is forming in a metastable precipitate appearing during the structural change, and that the subsequent change is characterized by the development of the other reflections in the pattern. This suggests that the presence of 12 reflections with a pseudo-12-fold symmetry must be a key factor in the formation of the σ structure. With this suggestion, we reproduced the micrograph in (d) from the experimental micrograph in (a), by using only the 12 reflections indicated by the solid arrows in (b). In (d), interestingly, the calculated micrograph exhibits a characteristic contrast, in addition to bright dots corresponding to center positions of CN14 columns. Furthermore, the comparison with the $[001]_\sigma$ projection of the σ structure in the inset indicates that although projected positions of atoms in icosahedral atomic clusters marked by the yellow-color regions cannot be sufficiently separated, as indicated by the open arrows, the contrast in (d) is basically identical to that in the projection. In other words, calculated micrographs reproduced by using the 12 reflections can give us enough information of the σ structure. Based on this result, in our study we have obtained the detailed features of the formation process of the σ structure by using calculated micrographs that were reproduced from experimental micrographs as original ones.

A metastable state appearing in the early stage of the (bcc $\rightarrow \sigma$) structural change is characterized by the presence of the 12 reflections, which were arranged with a pseudo-12-fold symmetry in $[001]_\sigma$ electron-diffraction patterns. This fact leads to the possibility that in diffraction patterns the structural change starts with the appearance of these 12 reflections. To check this possibility, we examined the crystallographic features of a bcc matrix near a metastable precipitate. Figure 5 shows three electron-diffraction patterns of different bcc matrixes near metastable precipitates, which were finally converted into three σ precipitates belonging to the (I), (II), and (III) groups, respectively. Their electron incidences are parallel to the (a) $[113]_{bcc}$, (b) $[111]_{bcc}$, and (c) $[110]_{bcc}$ directions. In these patterns, surprisingly, there basically exist 12 weaker reflections with a pseudo-12-fold symmetry, in addition to stronger reflections due to the bcc matrix. It is also found that two and six reflections among these 12 reflections are located very near the positions of 110_{bcc}-type reflections in (a) and (c), and (b), respectively. Another notable feature is that two more sets of 12 reflections with pseudo-12-fold symmetries can also be detected at higher scattering angles, as indicated by the solid and open arrows. We thus believe that these reflections with the pseudo-12-fold symmetries provide experimental evidence for the appearance of a dodecagonal atomic column. Based on this result, it seems to us that the (bcc $\rightarrow \sigma$) structural change in the Cr-Co alloy system starts with the appearance of dodecagonal atomic columns in a bcc matrix.

The above-mentioned experimental data suggest that the formation of the σ structure from the bcc structure may occur via the metastable state consisting of dodecagonal atomic columns. The five orientation relations would be a result of the structural change from the metastable dodecagonal-column state to the σ structure. In addition, our experimental data indicate that in the cases of the different orientation relations in the same group, the (bcc $\rightarrow \sigma$) structural changes basically exhibit the same crystallographic features. Based

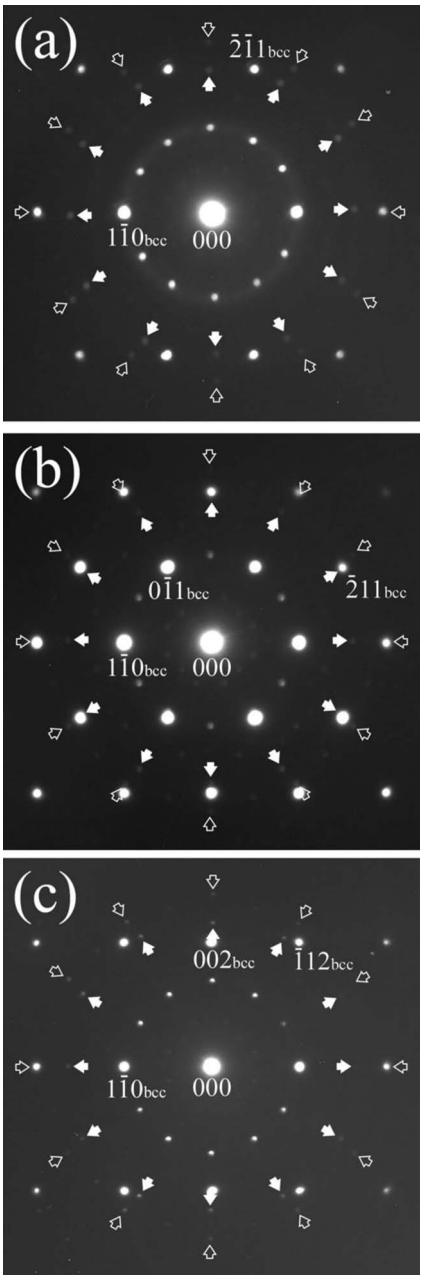

FIG. 5. Electron-diffraction patterns obtained from bcc matrixes near three different metastable precipitates belonging to the (I), (II), and (III) groups. These patterns were taken from alloy samples annealed at 1173 K for 10 min, and the metastable precipitates exhibiting the patterns in (a), (b), and (c) belong to the (I), (II), and (III) groups, respectively. The electron incidences in (a), (b), and (c) are then parallel to the $[113]_{bcc}$, $[111]_{bcc}$, and $[110]_{bcc}$ directions. In addition to 12 reflections at $\sin\theta/\lambda \approx 2.44$ nm^{-1}, in these patterns, two more sets of 12 reflections with a pseudo-12-fold symmetry can be detected at higher scattering angles, as indicated by the solid and open arrows.

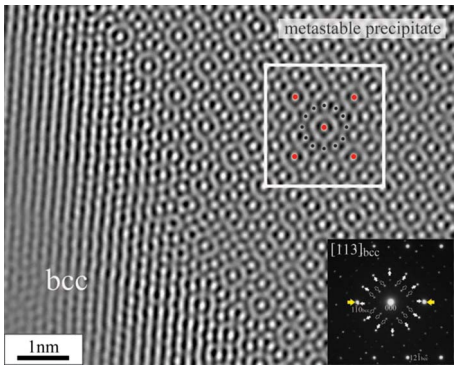

FIG. 6. (Color online) Calculated micrograph and a corresponding $[113]_{bcc}$ electron-diffraction pattern of a boundary region between a bcc matrix and a metastable precipitate in an alloy sample annealed at 1173 K for 10 min. Note that the metastable precipitate appeared during the structural change in the (I) group. The calculated micrograph was reproduced by using the 12 reflections marked by the white arrows in the pattern. A regular array of dodecagonal atomic columns having two shells is clearly seen in the metastable precipitate, as indicated in the area surrounded by the white lines. This suggests that the DACL state is formed in the metastable state.

on this fact, we describe below the detailed features of three structural changes which were found in the (I), (II), and (III) groups.

Figure 6 shows a calculated micrograph and a corresponding electron-diffraction pattern of the boundary regions between a bcc matrix and a metastable precipitate in an alloy sample annealed at 1173 K for 10 min. The (IA) orientation relation in the (I) group is finally satisfied in this case. The electron incidence of both the micrograph and the pattern is parallel to the $[113]_{bcc}$ direction, and the micrograph is reproduced by using 12 reflections indicated by the solid arrows in the pattern. In addition, two of the 12 reflections are present very near the positions of two 110-type bcc reflections marked by the yellow arrows. From the involvement of these two bcc reflections in reproducing the calculated micrograph, $(1\bar{1}0)_{bcc}$ lattice fringes are seen in the bcc matrix that exists on the left side of the calculated micrograph. On the right side where a metastable precipitate is present, on the other hand, we can observe a very interesting contrast, in particular, in the square area surrounded by the white lines. The contrast appears different from that of the σ structure in Fig. 4(d). The notable feature of the contrast is that we can find a structural unit having a pseudocentral symmetry in the contrast. When we look at one structural unit located at the center of the square area, it is understood that the unit has two shells around a red center dot, and that, around the center dot, the outer and inner shells exhibit the arrangement of 12 black-marked dots with a pseudo-12-fold symmetry and a ringlike contrast, respectively. Based on these features, the structural unit should be identified as a dodecagonal atomic column having two shells. The most important point is that this dodecagonal atomic column is entirely different from a CN14 column predicted from the σ structure reported in Sec. I. In the square area we can detect a regular array of dodecagonal atomic columns, as indicated by the red-marked dots. Based on this, as an ideal case, the metastable state in the early stage of the $(bcc \rightarrow \sigma)$ structural change may be referred to as the dodecagonal-atomic-column lattice (DACL) state. In addition to the 12 reflections with a pseudo-12-fold symmetry, in the diffraction pattern, the DACL state is characterized by the presence of reflections at lower scattering angles, which are indicated by the open arrows in the inset. It is likely that an increase in intensities of these reflections should reflect the spatial development of DACL regions.

Figure 7 shows a series of calculated micrographs indicating the $(bcc \rightarrow \sigma)$ structural change in the (IA) relation of the (I) group, together with corresponding electron-diffraction patterns. Four experimental micrographs as original ones before the reproduction were taken from (a) the starting bcc matrix including dodecagonal atomic columns, (b) the DACL state, (c) the $(DACL \rightarrow \sigma)$ transitional state, and (d) the final σ precipitate. The electron incidences for a pair of the patterns with a prime and a double prime in each state are, respectively, parallel and perpendicular to a column axis of a dodecagonal atomic column. Note that a column axis of a dodecagonal column is parallel to the $[001]_{\sigma}$ direction, and that a dodecagonal atomic column found here is distinct from a CN14 column suggested in Sec. I. It is understood from these micrographs and patterns that the $(bcc \rightarrow \sigma)$ structural change occurs in three steps; that is, (1) the appearance of dodecagonal atomic columns, (2) the formation of the DACL state, and (3) the subsequent $(DACL \rightarrow \sigma)$ structural change. In particular, the striking features of the change are that dodecagonal atomic columns appeared locally in the bcc matrix, and that steps (2) and (3) took place in a metastable precipitate. Among these three steps, the orientation relationship between the bcc and σ structures is directly associated with the later $(DACL \rightarrow \sigma)$ structural change. Note that the $(DACL \rightarrow \sigma)$ change is characterized by the formation of icosahedral atomic clusters in the DACL state, as will be discussed later. In addition, a period of the atomic column along a column axis was estimated to be about $11d_{bcc}(226)$ on the basis of the locations of two reflections indicated by the arrows in (a″). Note that $d_{bcc}(226)$ is a planar spacing of the $(226)_{bcc}$ plane of the bcc structure. The important point to note here is that these two reflections are also present in (d″) for the σ structure. Because the c-axis length of the σ structure is only about 5.1% smaller than $11d_{bcc}(226)$, the period of the σ structure along the c axis is basically established in the formation of a dodecagonal atomic column. This suggests that a structural unit of a dodecagonal atomic column along a column axis consists of four layers, and basically has the same length as the c-axis one of the σ structure.

The crystallographic features of the $(bcc \rightarrow \sigma)$ structural change in the (II) group are described below. In the (II) group, there is only the (IIA) orientation relation of $[111]_{bcc} \| [001]_{\sigma}$ and $(1\bar{1}0)_{bcc} \| (3\bar{3}0)_{\sigma}$. Figure 8 shows a calculated micrograph and a corresponding $[111]_{bcc}$ electron-diffraction pattern of an annealed sample in an early stage of the structural change. Both the micrograph and the pattern were taken from the same boundary region between a bcc matrix and a metastable precipitate. The point to note here is that the contribution of six 110_{bcc}-type reflections due to the

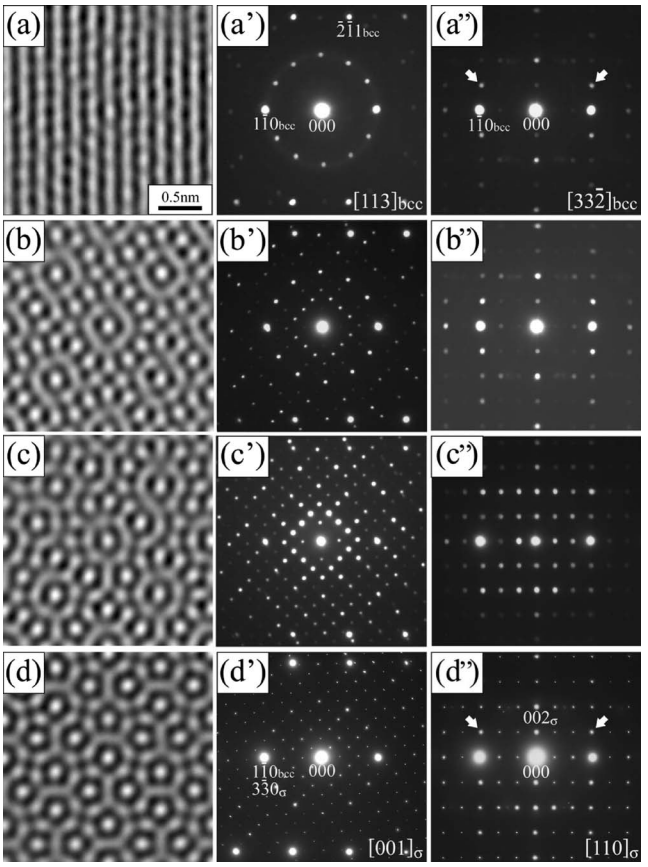

FIG. 7. Series of both calculated micrographs and corresponding electron-diffraction patterns indicating the (bcc $\rightarrow \sigma$) structural change in the (I) group. The original experimental micrographs and the corresponding patterns were obtained from the bcc state involving dodecagonal atomic columns for (a), (a′), and (a″), the DACL state for (b), (b′), and (b″), the transitional state during the (DACL $\rightarrow \sigma$) structural change for (c), (c′), and (c″), and the σ state for (d), (d′), and (d″). In this experiment, alloy samples annealed at 1173 K for 10 min and 24 h were used for the experimental data of the bcc, DACL, and transitional states, and the σ state, respectively. Both the micrograph and the patterns of the DACL state were, in particular, taken from a boundary region of a metastable precipitate near a bcc matrix. In addition, the electron incidences of the patterns with a prime and a double prime in each state are, respectively, parallel and perpendicular to a column-axis direction. Note that the column-axis direction in the (I) group is obviously parallel to the $[113]_{bcc}$ direction in the bcc matrix. The contrast reflecting the formation of icosahedral atomic clusters can be detected in the transitional state shown in (c).

bcc matrix is also involved in the calculated micrograph. This is because these bcc reflections are very closely located at six of 12 reflections due to a dodecagonal atomic column, as indicated by the yellow arrows in the pattern. Three $\{110\}_{bcc}$-type lattice fringes and bright dots as their intersections are actually seen in the bcc matrix, the left side of the micrograph, while the metastable precipitate on the right side exhibits the characteristic contrast representing dodecagonal atomic columns. As shown in the square area surrounded by the white lines, the metastable state can be identified as the DACL state, just as in the case of the (I) group. Furthermore,

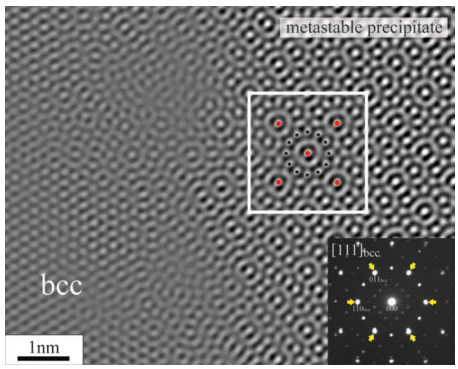

FIG. 8. (Color online) Calculated micrograph and a corresponding $[111]_{bcc}$ electron-diffraction pattern of a boundary region between a bcc matrix and a metastable precipitate in the case of the (II) group. Both the experimental micrograph and the pattern were taken from a sample annealed at 1173 K for 10 min. A bcc matrix and a metastable precipitate are, respectively, present on the left and right sides of the micrograph. Although a change in the contrast related to the formation of icosahedral atomic clusters partially occurs in the metastable precipitate, we can see the DACL state, in particular, in the square area surrounded by the white lines.

the interesting contrast reflecting the formation of the DACL state is seen in the boundary region of the metastable precipitate. That is, it is understood that the (bcc $\rightarrow \sigma$) structural change in the (II) group also occurred via the DACL state.

A series of calculated micrographs for the (bcc $\rightarrow \sigma$) structural change in the (II) group is shown in Fig. 9, together with corresponding electron-diffraction patterns. The micrographs in (a), (b), (c), and (d) were, respectively, obtained from the bcc state involving dodecagonal atomic columns, the DACL state, the (DACL $\rightarrow \sigma$) transitional state, and the σ state. The patterns with a prime and a double prime in each state have the electron incidences parallel and perpendicular to a column axis of the dodecagonal atomic column. A regular array of bright dots identified as intersections of three $\{110\}_{bcc}$ fringes is clearly seen in the bcc matrix of (a), and the DACL state is formed in (b). The σ structure then appears from the DACL state by forming icosahedral atomic clusters in the DACL state. From the diffraction pattern in (a″), as indicated by the two arrows, it is also found that a period of a dodecagonal atomic column along a column axis is almost identical to the c-axis length of the σ structure. That is, we can understand that there is no difference between the structural changes in the (I) and (II) groups. As shown in Fig. 10, furthermore, the structural change in the (III) group is exactly the same as those in the (I) and (II) groups. In other words, the (bcc $\rightarrow \sigma$) structural changes in the (I), (II), and (III) groups can commonly be expressed as the bcc structure $\rightarrow$ (1) the appearance of dodecagonal atomic columns $\rightarrow$ (2) the formation of the DACL state $\rightarrow$ (3) the formation of icosahedral atomic clusters $\rightarrow$ the σ structure. It should be noted that the formation of icosahedral atomic clusters in the DACL state took place in a metastable precipitate, while dodecagonal atomic columns were already present in a bcc matrix.

In the (bcc $\rightarrow \sigma$) structural change via the DACL state, the latter (DACL $\rightarrow \sigma$) change is characterized by the formation

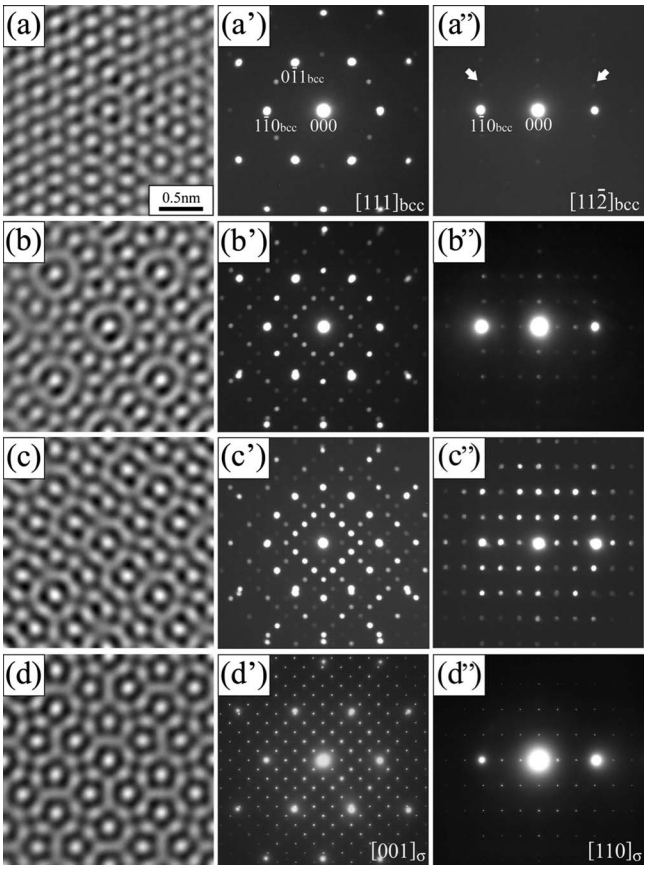

FIG. 9. Series of both calculated micrographs and corresponding electron-diffraction patterns indicating the (bcc→σ) structural change in the (II) group. The experimental data were collected from the bcc state involving dodecagonal atomic columns for (a), (a′), and (a″), the DACL state for (b), (b′), and (b″), the transitional state during the (DACL→σ) structural change for (c), (c′), and (c″), and the σ state for (d), (d′), and (d″). The experimental conditions such as the annealing condition for sample preparation are the same as those in the (i) group of Fig. 7. In the case of the (II) group, however, the electron incidence of both the micrograph and the pattern with a prime in each state is parallel to the $[111]_{bcc}$ direction in the bcc matrix, while the pattern with a double prime has the electron incidence perpendicular to it.

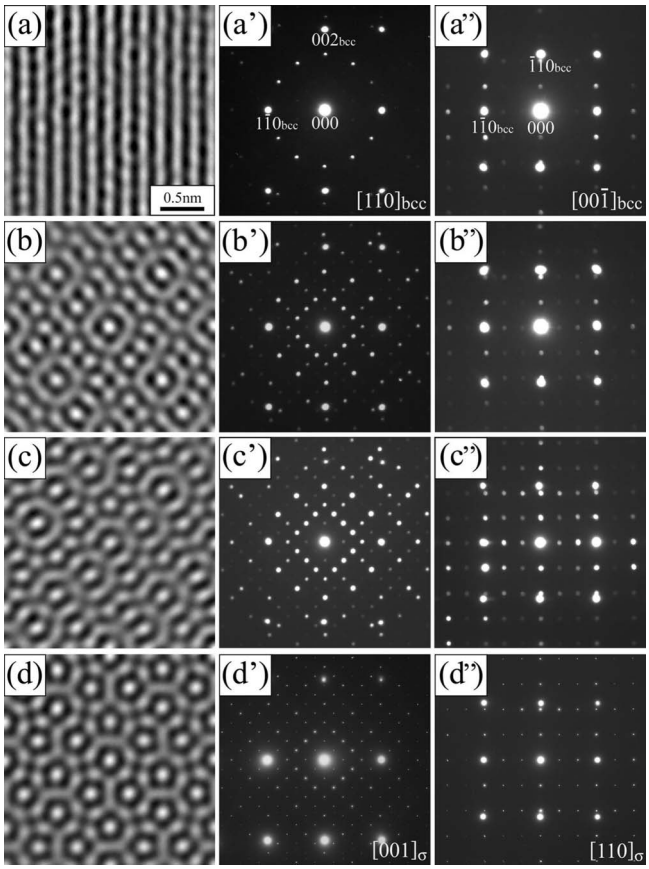

FIG. 10. Series of both calculated micrographs and corresponding electron-diffraction patterns for the (bcc→σ) structural change in the (IIIA) relation of the (III) group. The experimental micrographs and the patterns are taken from the bcc state involving dodecagonal atomic columns for (a), (a′), and (a″), the DACL state for (b), (b′), and (b″), the transitional state during the (DACL→σ) structural change for (c), (c′), and (c″), and the σ state for (d), (d′), and (d″). The experimental conditions to obtain the micrographs and the patterns are the same as those in the (I) and (II) groups, except for the electron incidence. In the (III) group, the incidence of both the micrograph and the pattern with a prime in each state is parallel to the $[110]_{bcc}$ direction in the bcc matrix, that is, the column-axis direction.

of icosahedral atomic clusters in the DACL state. As a result of the later change in the (I) group, σ regions with two different orientation relations appeared in an equilibrium precipitate. For the (II) group with only one relation, on the other hand, complicated electron-diffraction patterns with the $[001]_{\sigma}$ electron incidence were often observed in equilibrium σ precipitates. Figure 11(a) is such a pattern obtained from a sample annealed at 1173 K for 24 h, together with a corresponding bright-field image in the inset. As seen from the image, a σ precipitate consists of several regions. Reflecting this, we see a lot of reflections in the pattern. The feature of the pattern is that sets of three reflections surrounded by the small circle are likely to be arranged with a pseudo-12-fold symmetry around the origin 000. This implies that the diffraction pattern should be interpreted as a superposition of diffraction patterns from three σ variants with the (IIA) relation of $[111]_{bcc}\|[001]_{\sigma}$ and $\{1\bar{1}0\}_{bcc}\|(3\bar{3}0)_{\sigma}$. We then calculated the $[001]_{\sigma}$ electron-diffraction pattern in (b) on the assumption that three variants have the relations of ① $(1\bar{1}0)_{bcc}\|(3\bar{3}0)_{\sigma}$, ② $(10\bar{1})_{bcc}\|(3\bar{3}0)_{\sigma}$, and ③ $(0\bar{1}1)_{bcc}\|(3\bar{3}0)_{\sigma}$. The calculated pattern actually reproduces the experimental one. Note that in the calculated pattern the reflections of the ①, ②, and ③ variants are, respectively, indicated by the black, red, and green dots. Based on this agreement, we believe that, in addition to the presence of the five orientation relations, the pattern involving the contribution of three variants in the (II) group is also experimental support for the fact that the later (DACL→σ) change is associated with the formation of icosahedral atomic clusters, as will be discussed later.

IV. DISCUSSION

The present experimental data reveal that in the (I), (II), and (III) groups, the (bcc→σ) structural changes resulting in

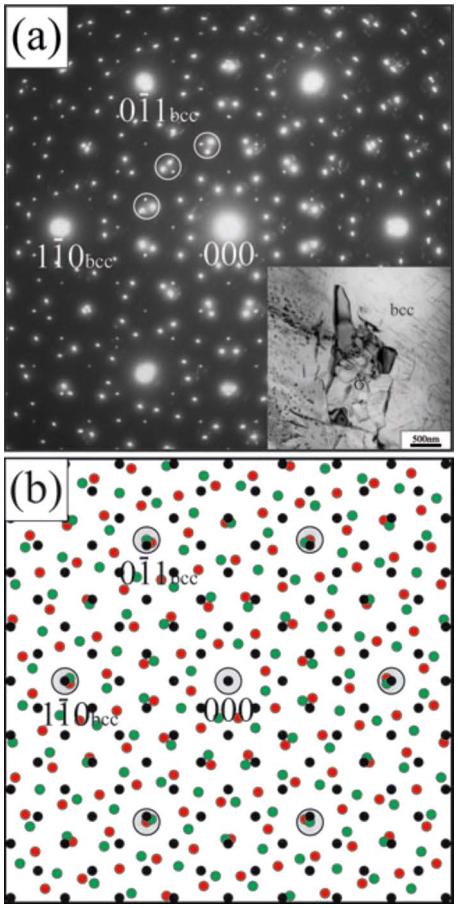

FIG. 11. (Color online) Electron-diffraction pattern and a corresponding bright-field image obtained from an equilibrium σ precipitate in an alloy sample annealed at 1173 K for 24 h, together with a calculated diffraction pattern. Because of the equilibrium σ precipitate in the (II) group, the electron incidence of the pattern and the image is parallel to the $[111]_{bcc}$ direction. Sets of three reflections surrounded by the small circle are arranged with a pseudo-12-fold symmetry in the pattern. The calculated pattern in (b) was thus reproduced by taking into account three σ variants with the (IIA) relation.

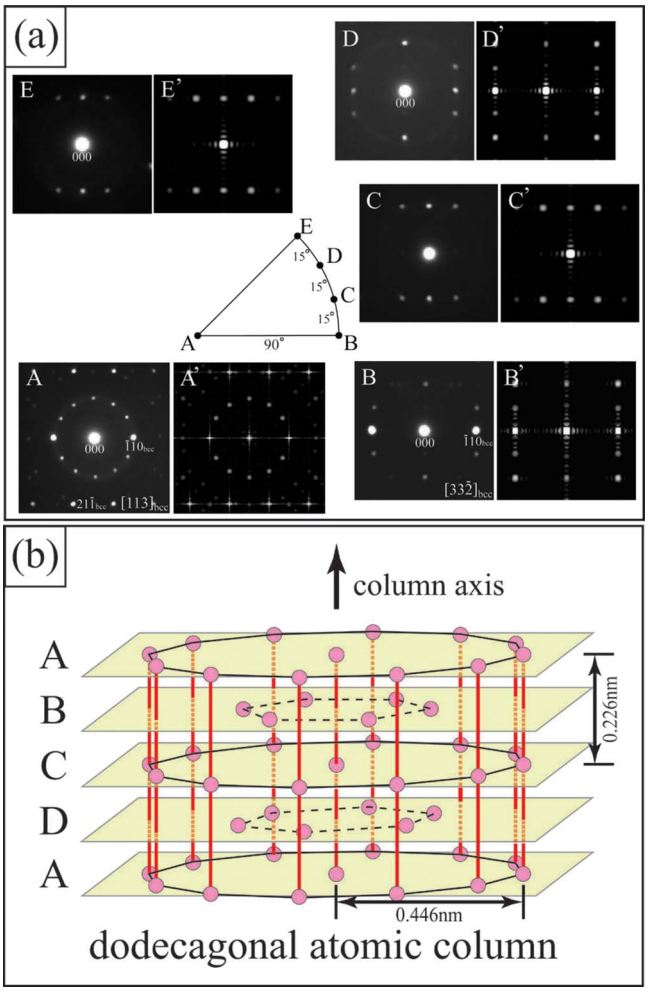

FIG. 12. (Color online) Experimental and calculated electron-diffraction patterns of a bcc matrix involving dodecagonal atomic columns, together with a schematic diagram showing a model of a structural unit of a dodecagonal atomic column. The electron incidences of the patterns are indicated by letters A, B, C, D, and E in a part of a pole figure at the center. The experimental pattern and a calculated one with a prime in each pair are, respectively, shown on the left and right sides. In (b), atoms in the structural unit of a dodecagonal atomic column are assumed to be identical to one another, and are denoted by the red circles.

the five orientation relations are essentially identical to one another. Specifically, the structural change involves the following three steps: (1) the appearance of dodecagonal atomic columns, (2) the formation of the DACL state, and (3) the formation of icosahedral atomic clusters in the DACL state. Note that a dodecagonal atomic column found here is distinct from a CN14 column predicted from the reported σ structure in Sec. I. In other words, the σ structure is produced by the formation of the icosahedral atomic cluster in the DACL state, and not directly from the bcc structure. Based on this, it is clear that the appearance of the five orientation relations between the bcc and σ structures is associated with the formation of icosahedral atomic clusters in the DACL state. In this discussion, then, we first propose a structural model of the dodecagonal atomic column having two shells, and next discuss atomic displacements for the formations of both a dodecagonal atomic column from the bcc structure and icosahedral atomic clusters in the DACL state. In addition to these, possible orientation relations and σ variants are also predicted on the basis of the atomic-displacement model for the formation of icosahedral atomic clusters in the DACL state.

We first construct the structural model of the dodecagonal atomic column that is consistent with the features of the observed electron-diffraction patterns. As shown in Fig. 5, interestingly, the diffraction patterns obtained from a bcc matrix near a metastable precipitate basically exhibit the 12 reflections arranged with a pseudo-12-fold symmetry around the origin 000, in addition to the bcc reflections. Because diffraction patterns of a bcc matrix involving dodecagonal atomic columns have the same features in all groups, for the (I) group, experimental and calculated patterns with five electron incidences are shown in Fig. 12(a), together with part of a pole figure. For each pair of the patterns in (a), there are the experimental and calculated patterns on the left and

right sides, respectively. Among the experimental patterns, first, the pattern exhibiting 12 reflections with a pseudo-12-fold symmetry are located at position A in the pole figure for the $[113]_{bcc}$ incidence parallel to a column axis. On the other hand, there are reflections, indicating a period of $11d_{bcc}(226)$, in the patterns at positions B and D. Note that location B corresponds to the $[33\bar{2}]_{bcc}$ incidence. At positions C and E, we can see only reflections with the spacing of a half of $11d_{bcc}(226)$. As mentioned earlier, the spacing of $11d_{bcc}(226)$ is almost the same as the c-axis length of a unit cell of the σ structure. This implies that the spacing of $11d_{bcc}(226)$ is almost unchanged during the subsequent structural change to the σ structure, as shown in Figs. 7, 9, and 10. In other words, a structural unit of the dodecagonal atomic column along a column axis should consist of four layers, just as in the case of the σ structure. Based on these features, in (b), we propose a structural model for a structural unit of the dodecagonal atomic column. The features of the proposed unit are that, in the A and C layers, 12 atoms are arranged with a pseudo-12-fold symmetry about a column axis, and that the positions of the 12 atoms in these two layers should be identical to one another. As a result of the same positions, there exist atomic bonds with the shortest length of about 0.226 nm along a column-axis direction in the structural unit, as indicated by the red vertical lines. On the other hand, six atoms with a pseudo-sixfold symmetry are present in the B and D layers. To keep a pseudo-12-fold symmetry in the projection along a column axis, further, positions of six atoms in the B layer need to be rotated 30 degrees from those in the D layer about a column axis. We then calculated electron-diffraction patterns on the basis of this structural model. In the calculation, column clusters consisting of nine dodecagonal atomic columns with three structural units along a column axis were uniformly distributed in a bcc matrix. For each pair, the calculated pattern corresponding to the experimental one on the left side is shown on the right side. The comparison between the experimental and calculated patterns clearly indicates that the calculated patterns correspond well to the experimental ones. This implies that the structural model in (b) is appropriate for a structural unit of the dodecagonal atomic column found in this study.

Based on the structural model we determined for the dodecagonal atomic column, we discuss here an atomic displacement from the bcc structure to the dodecagonal atomic column in the (I), (II), and (III) groups. It should be noted that because a unique crystallographic direction of the dodecagonal column is obviously a column axis, there exists only one atomic displacement for the formation of the dodecagonal column in each group. Figure 13 shows three types of atomic displacements for the (I), (II), and (III) groups, in which atomic shifts are indicated by the red arrows. Notice that the number of layers in the bcc structure that are needed to form a structural unit of a dodecagonal column is different; that number is, 11 layers of the $(226)_{bcc}$ plane in the (I) group, 6 layers of the $(222)_{bcc}$ plane in the (II) group, and 2 layers of the $(110)_{bcc}$ plane in the (III) group. Among these three types of atomic displacements, first, the displacement for the (I) group is depicted in the upper diagram. As seen in the diagram, the dodecagonal atomic column can easily be formed by simple atomic shifts. The notable feature in the (I) group is that the formation needs the introduction of atomic vacancies marked by the green open squares in the Ia and Ih layers. As for the (II) group, in the middle, it is understood that atomic shifts are very simple. Specifically, three neighboring $(222)_{bcc}$ layers are rearranged into two layers in the dodecagonal atomic column. Furthermore, in the lower diagram for the (III) group every $(110)_{bcc}$ layer is separated into two layers. Then, 12 atoms sit on one layer and the other layer has six atoms. The points to note here are that the introduction of both an atomic vacancy and an additional atom is not needed in the (II) and (III) groups, and that the relatively large shifts occur in the (III) group. In addition, a lattice contraction along a column axis is involved in the (I) and (II) groups, while the atomic shifts in the (III) group accompany a lattice expansion.

In the latter (DACL$\rightarrow\sigma$) change of the (bcc$\rightarrow\sigma$) structural change, our experimental data suggest that icosahedral atomic clusters were formed in the DACL state. In other words, a CN14 column is produced as a result of the formation of icosahedral atomic clusters. This implies that, instead of a CN14 column as suggested in Sec. I, an icosahedral atomic cluster should be a structural unit of the σ structure. Now we discuss the atomic displacement for the appearance of icosahedral clusters in the DACL state. Figures 14(a) and 14(b) are, respectively, the three-dimensional schematic diagrams showing atomic shifts for two types of icosahedral atomic clusters, and the projections of the atomic positions of the DACL state and the σ structure to show the atomic displacement in the later (DACL$\rightarrow\sigma$) change. Note that the projecting directions in (b) are parallel to the column-axis and perpendicular directions for the DACL state and the $[001]_\sigma$ and $[33\bar{2}]_\sigma$ directions for the σ structure, and that, in the σ structure, the α-type icosahedral atomic cluster is rotated 90 degrees from the β-type one about the $[001]_\sigma$ direction. In (a), atomic shifts to form these two clusters for the (IA) case are indicated by the red arrows. It is known that in (a) the α-type and β-type icosahedral clusters can be formed by simple atomic shifts mainly along a column axis. The important points are that the introduction of a vacancy and an additional atom is not needed in the formation of these icosahedral clusters, and that no new layer is produced by the atomic shifts. Of these two types of icosahedral clusters, further, the α-type cluster is formed in the interior of one dodecagonal atomic column, while the β-type cluster needs three columns. Because both clusters are formed by atomic shifts mainly along the column axis, projected atomic shifts in the (DACL$\rightarrow\sigma$) change are extremely simple in the $[001]_\sigma$ projection, as shown in (b). Thus we know that when the metastable DACL state is taken into account, the (bcc$\rightarrow\sigma$) structural change can be explained by using very simple atomic shifts.

The appearance of both the five orientation relations between the bcc and σ structures and the three σ variants in the (II) group is directly associated with the (DACL$\rightarrow\sigma$) structural change in the later stage. In particular, the higher symmetry of the dodecagonal atomic column about a column axis should be crucial for their appearance. Based on the atomic-displacement model mentioned above, we predict

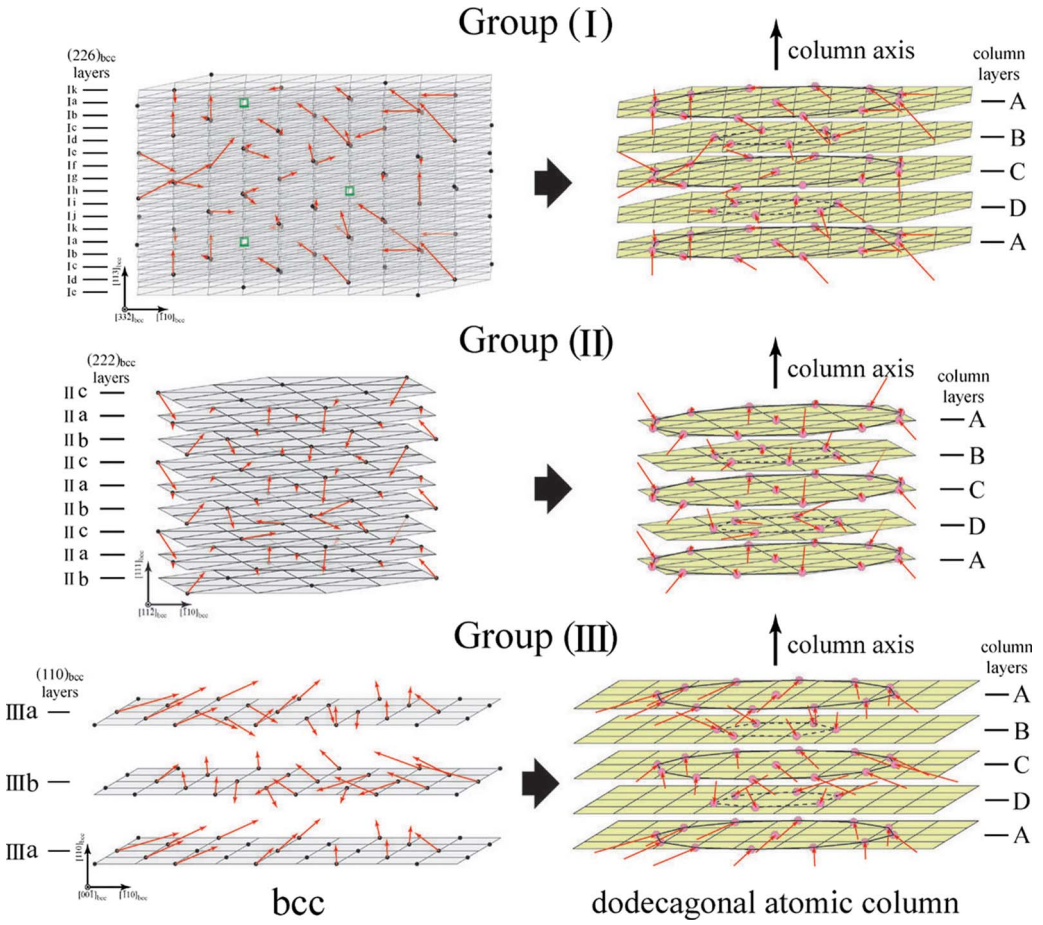

FIG. 13. (Color online) Schematic diagram showing three types of atomic displacements for the formation of a dodecagonal atomic column from the bcc structure in the (I), (II), and (III) groups. In each group, the bcc structure before atomic shifts, indicated by the red arrows, on the left side is converted into a dodecagonal atomic column after the shifts on the right side. The length of each red arrow represents the magnitude of an atomic shift.

possible orientation relations and σ variants and make comparison with the experimental results. Figure 15 shows the schematic diagrams indicating possible relations and σ variants for the (I), (II), and (III) groups. To easily understand the detailed features of the structural relation between the dodecagonal column and the σ structure, in the diagrams, we put on one starting dodecagonal column at a center and possible σ configurations with different orientations around it. We depict both the column-axis projection of the dodecagonal column and the $[001]_\sigma$ projections of possible σ configurations with different orientations. Here, when we pay attention to an α-type icosahedron marked by the yellow area in the diagram, it is understood that there are 12 possible σ configurations numbered ① to ⑫. Because the σ structure has a tetragonal symmetry, among the 12 configurations, we will discuss only three configurations numbered by ①, ②, and ③. In the case of the (I) group with the directional relation of $[113]_{bcc}\|[001]_\sigma$, when the planar relation of configuration ① is assumed to be $(1\bar{1}0)_{bcc}\|(3\bar{3}0)_\sigma$, configurations ② and ③ have the relations of $(1\bar{1}0)_{bcc}\|(4\bar{1}0)_\sigma$ and $(1\bar{1}0)_{bcc}\|(4\bar{1}0)_\sigma$. These configurations are then two σ variants with $(1\bar{1}0)_{bcc}\|(4\bar{1}0)_\sigma$. These variations suggest that there are two possible orientation relations of (IA) and (IB). Both of these were found experimentally. As for the (II) group with the relation of $[111]_{bcc}\|[001]_\sigma$, the configurations of ① and ③ have the relations of $(1\bar{1}0)_{bcc}\|(3\bar{3}0)_\sigma$ and $(0\bar{1}1)_{bcc}\|(3\bar{3}0)_\sigma$, respectively, and are two variants. For configuration ③, we have the relation of $(1\bar{1}0)_{bcc}\|(4\bar{1}0)_\sigma$. However, this relation is equivalent to $(10\bar{1})_{bcc}\|(330)_\sigma$. Then, only one relation of (IIA) $[111]_{bcc}\|[001]_\sigma$ and $(1\bar{1}0)_{bcc}\|(3\bar{3}0)_\sigma$ is present in the (II) group. Furthermore, in this case there are three sets of configurations, (①, ④, ⑦, ⑩), (②, ⑤, ⑧, ⑪), and (③, ⑥, ⑨, ⑫). Since each set gives rise to the same electron-diffraction pattern, we regard one set as one variant, and can expect a $[001]_\sigma$ electron-diffraction pattern that consists of the superposition of diffraction patterns from three σ variants. Such a pattern was actually observed and is shown in Fig. 11. In addition, the situation of the (III) group is identical to that of the (I) group. This implies that two relations of (IIIA) $[110]_{bcc}\|[001]_\sigma$, $(1\bar{1}0)_{bcc}\|(3\bar{3}0)_\sigma$ and (IIIB) $[110]_{bcc}\|[001]_\sigma$, $(1\bar{1}0)_{bcc}\|(4\bar{1}0)_\sigma$ are possible in the (III) group. This leads us to the understanding that the presence of the five orientation relations and three σ variants in the (II) group, which were found experimentally, can be explained consistently in terms of the atomic-displacement model shown in Fig. 14.

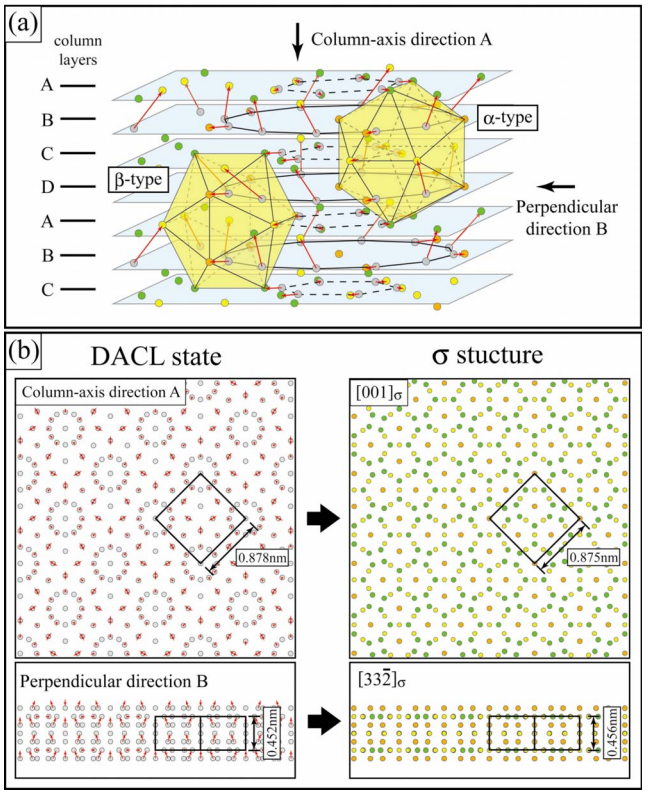

FIG. 14. (Color online) (a) Schematic diagram showing atomic shifts for the formation of icosahedral atomic clusters in the DACL state, and (b) the projections of the DACL state and the σ structure to show atomic shifts in the (DACL$\rightarrow\sigma$) structural change. The red arrows in (a) and (b) denote atomic shifts, and the length of each arrow corresponds to the magnitude of a shift. It is understood that the size of the unit cell in the DACL state is almost identical to that of the σ structure, as indicated by the black lines in (b).

We finally discuss the physical origin of the formation of the metastable dodecagonal atomic column in the (bcc$\rightarrow\sigma$) structural change. To characterize the dodecagonal atomic column shown in Fig. 12(b), we estimate bond lengths between two neighboring atoms in the structural unit of the dodecagonal column. A careful analysis of bond lengths indicates that the shortest bonds have a bond length of about 0.226 nm along a column axis, as indicated by the red vertical lines in Fig. 12(b). Because the shortest bond length between two neighboring atoms in a bcc structure is about 0.246 nm, the reduction in bond length in the formation of the dodecagonal atomic column is surprisingly estimated to be about 8.1%. One of possible mechanisms for the reduction in bond length may be the formation of an atomic bond with covalent character in a metallic bcc matrix. Although other mechanisms are also possible, we now believe that the appearance of a dodecagonal atomic column is associated with the formation of the shortest atomic bonds presumably with covalent character along a column axis. It should be noted that this situation is very similar to that for decagonal atomic columns consisting of icosahedral atomic clusters in the Laves structures.[13,14]

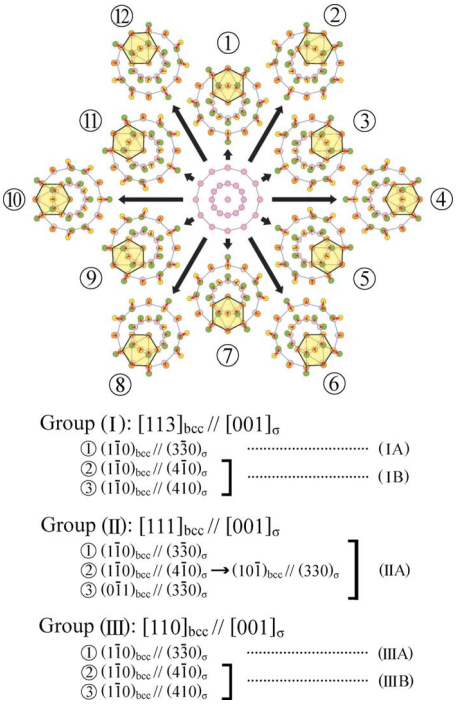

FIG. 15. (Color online) Schematic diagram indicating 12 possible σ configurations produced from one dodecagonal atomic column by the formation of an icosahedral atomic cluster in the (I), (II), and (III) groups. The resultant orientation relations in these groups are listed below. In the upper diagram, the yellow area in each σ configuration represents the A-type icosahedral cluster that is formed in the (DACL$\rightarrow\sigma$) structural change.

V. CONCLUSIONS

The crystallographic features of the (bcc$\rightarrow\sigma$) structural change in the (bcc$\rightarrow$bcc+σ) reaction in the Cr-Co alloy system have been investigated by transmission electron microscopy. The present experimental data clearly reveal that the structural change occurred via the metastable state consisting of dodecagonal atomic columns having two shells, which are distinct from CN14 columns. In the electron-diffraction patterns, the metastable state is characterized by 12 reflections arranged with a pseudo-12-fold symmetry around the origin 000. The interesting features are that dodecagonal atomic columns already appear locally in a bcc matrix, and that dodecagonal columns form the DACL state in the metastable precipitate. As a result of the presence of the DACL state, the σ structure is produced by the formation of icosahedral atomic clusters in the DACL state. This implies that the structural unit of the σ structure is not a CN14 column, but an icosahedral atomic cluster, that is, a CN12 polyhedron. In addition, the (DACL$\rightarrow\sigma$) structural change in the later stage results in both the five orientation relations between the bcc and σ structures and the three σ variants in the (II) group. In fact, both the relations and the variants found experimentally are explained quite well by using the atomic-displacement model for the formation of icosahedral atomic clusters in the DACL state.

[1] E. C. Bain and W. E. Griffiths, Trans. AIME **75**, 166 (1927).
[2] P. Chevenard, J. Inst. Met. **37**, 471 (1927).
[3] F. Adcock, J. Iron Steel Inst., London **124**, 99 (1931).
[4] P. Duwez and H. Martens, *Ductile Chromium and Its Alloys* (American Society Metals, Cleveland, 1957), p. 322.
[5] M. B. Cortie, I. Wolff, K. Premachandra, M. Tullmin, and E. A. Demarsh, *Proceedings of the Stainless Steels Conference* (The Iron and Steels Institute of Japan, Tokyo, 1991), p. 555.
[6] P. I. Kripyakevich, *A Systematic Classification of Types of Intermetallic Structures* (Consultants Bureau, New York, 1964).
[7] K. Schubert, *Kristallstrukturen Zweikomponentiger Phasen* (Springer-Verlag, Berlin, 1964).
[8] S. Samson, in *Structural Chemistry and Molecular Biology*, edited by A. Rich and N. Davidson (Freeman, San Francisco, London, 1969).
[9] W. B. Pearson, *The Crystal Chemistry and Physics of Metals and Alloys* (Wiley, New York, 1972).
[10] A. Hirata, A. Iwai, and Y. Koyama, Phys. Rev. B **74**, 054204 (2006).
[11] T. Doi, M. Tanimura, and Y. Koyama, Phys. Rev. B **77**, 134205 (2008).
[12] G. J. Dickins, A. M. B. Douglas, and W. H. Taylor, Acta Crystallogr. **9**, 297 (1956).
[13] A. Hirata, Y. Koyama, and M. Tanimura, Phys. Rev. B **67**, 144107 (2003).
[14] A. Hirata and Y. Koyama, Phys. Rev. B **70**, 134203 (2004).
[15] C. Allibert, C. Bernard, N. Valigmat, and M. Dombre, J. Less-Common Met. **59**, 211 (1978).
[16] K. Ishida and T. Nishizawa, Bull. Alloy Phase Diagrams **11**, 4 (1990).